Ferritic-martensitic structure in steel hardenable by copper precipitation

J Dlouhy, T Studecky and P Podany

COMTES FHT a.s., Průmyslová 995, 334 41, Plzeň, Czech Republic

E-mail: jaromir.dlouhy@comtesfht.cz

Abstract. The copper precipitation offers possibility of effective and easily achievable ferrite strengthening. There is reported yield point rise by 150 MPa thanks to formation of nanometric copper precipitates in ferrite for Cu content 1.5 wt.%. Such rise of yield strength is most significant for soft and ductile materials, containing free ferrite. Ferritic-martensitic dual steels are example of such material. They are widely used for their favourable combination of strength and ductility. Their yield strength is defined by the soft phase, the ferrite. Ferrite strengthening in these steels is achieved mainly by grain refinement and by solution strengthening caused by substitutional alloying elements. This article describes preparation of dual phase structure in 0.2% C steel alloyed by Cu, Mn, Ti and B. Dual phase structure was prepared by controlled rolling with rolling finishing temperatures in the intercritical region. Samples were analysed by light and scanning electron microscopy. Hardness was measured and tensile tests were performed.

1 Introduction

Copper precipitation is widely studied mean of strengthening ferrite [1 – 4]. Solubility of copper in ferrite decreases with temperature. Copper can precipitate from supersaturated ferrite solution when its concentration rises above 0.5 wt. %. Nanometer-size copper precipitates can strengthen ferrite and increase tensile strength and yield point of steel. Micro alloying by boron and titanium was reportedly successful approach in experiments seeking the most effective way for copper precipitation and structural refinement during thermomechanical processing [5, 6]. Boron increases hardenability and copper suppresses formation of pearlite during continuous cooling. These effects facilitates formation of ferritic-martensitic structure. Titanium is added as binding agent for nitrogen, because nitrogen can form boron nitride and remove in such way boron from solid solution.

This article is devoted to the preparation and annealing of dual ferritic-martensitic structure of copper alloyed steel. Dual F/M steels are widely used as structural steels combining high-strength with sufficient formability and ductility. Their yield strength is limited by yield strength of their weaker constituent – ferrite. Copper precipitation can offer strengthening of the ferrite and thus enhancement of the yield stress of F/M microstructure.

2 Experiment

2.1 Material preparation

Two experimental melts were casted in vacuum induction furnace – lower (“L” melt) and higher (“H” melt) alloyed by copper and manganese. Their chemical composition is in the Table 1. The melts do not differ in content of other elements.

Casted ingots weighing 500 kg were hot forged by hydraulic press into slabs 300 x 80 mm in crossection. The slabs were hot rolled into sheets 30 mm thick. Rolling mill in duo configuration was used with 550 mm rolls diameter and rolling speed 1 m/s. Forging and rolling temperature was 1050°C.

30 mm thick sheets were cut into samples 150 mm wide and 250 mm long. They were milled into thickness 25 mm to remove decarburized layer.

Temperatures A1 and A3 were determined by dilatometric measurement. Samples were 20 mm long and 4 mm in diameter. Both heating and cooling rates were 3 °C/min. There was significant difference between temperatures $Ac_{1,3}$ during heating and temperatures $Ar_{1,3}$ during cooling, as can be expected due to the boron content. Temperature Ar_1 for the melt H could not even be determined, because proeutectoid ferrite formation was followed by bainitic transformation. Thus temperatures $Ac_{1,3}$ will be close to the equilibrium temperatures $A_{1,3}$ and temperatures $Ar_{1,3}$ illustrates stability of austenite. Transformation temperatures are in the Table 1.

Table 1. Chemical composition and temperatures Ac_1, Ac_3, Ar_1, Ar_3 of the experimental materials. Concentrations in wt. %.

Melt	C	Mn	Cu	Si	Ti	B	N	Ac3 [°C]	Ac1 [°C]	Ar3 [°C]	Ar1 [°C]
L	0.21	0.98	1.08	0.08	0.025	0.0013	0.0063	812	719	779	629
H	0.21	2.00	1.49	0.08	0.023	0.0015	0.0057	779	695	691	-

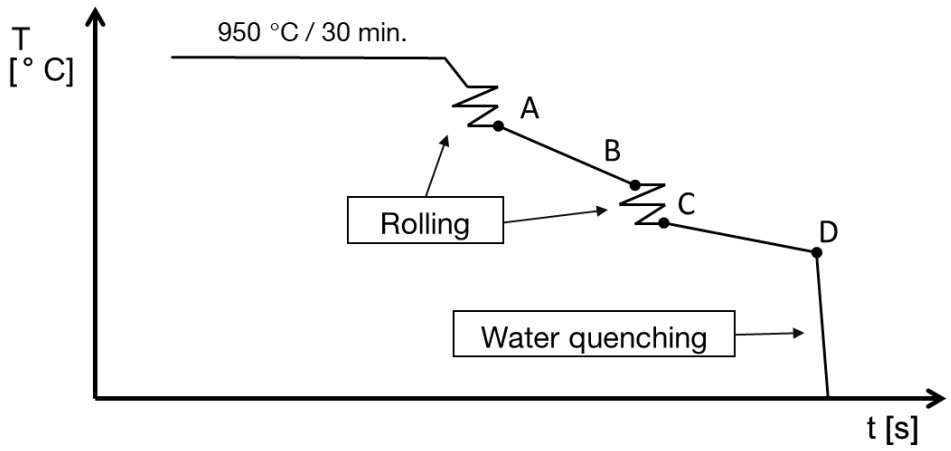

Figure 1. Schematic description of the cotrolled rolling regime.

Table 2. Regimes of controlled rolling.

Regime	A	B	C	D
L 1	830	800	730	680
L 2	830	760	690	650
H 1	830	800	730	700
H 2	830	740	680	650

2.2 Controlled rolling and thermal treatment

The controlled rolling was performed by rolling mill described in the section 2.1. Samples were covered by protective coating against decarburization and heated in atmospheric furnace. The scheme of the experimental rolling is in the Figure 1. Heating temperature was 950°C, dwell at the temperature was 30 minutes.

First part of the controlled rolling simulated conventional hot rolling. The rolling operation above point A consisted of two passes through the rolling mill wit summary reduction of 50%. Thickness of the sample in point A was 12.5 mm, temperature 830°C. Sample was cooled in still air until it reached the temperature for the second intercritical rolling operation (see in Table 2). This second rolling consisted in three passes with summary reduction of 55% into final thickness 5.6 mm. Sample was transferred into cooling tunnel and rapidly cooled by water spraying. Delay between intercritical rolling and water spraying was 10 seconds.

Two regimes were performed for each material. Regime 1 included rolling above A_1 temperature, but mainly or entirely under temperature A_3. Regime 2 included rolling around A_1 temperature. Specimens for tensile testing was machined from the samples. Three specimens were tested in as-rolled conditions, three samples were annealed at 400 °C for 1 hour.

2.3 Sample characterization

Flat specimens for tensile testing were machined from samples in as-rolled state and annealed state. The specimens had gauge length 45 mm, width 8 mm and thickness of the sample – from 5,3 to 5,6 mm. Ultimate tensile strength (UTS), yield stress (YS), homogeneous plastic deformation (Ag), ductility (A5) and reduction of area (Z) were measured. YS was determined as proof stress at 0.2 % offset. In case of distinctive yield point the upper yield point was determined as YS.

Metallographic analysis was performed on the sections prepared in longitudinal direction. Section were mechanically ground and polished. Microstructure was revealed by 3 % Nital solution. Microstructure was observed by light microscope and scanning electron microscope. Phase composition was roughly estimated on the base of the image analysis. Exact measurement was not possible due to heterogeneity and small grain size in some areas. Values given in following chapter are orientation values with estimated uncertainty ±10 vol.%.

3 Results and Discussion

Tensile test results of the as-rolled specimens are in Table 3. Both materials showed significant deformation hardening. There was large difference between strength of both materials. Material 2 had UTS and YS higher by approx. 500MPa and its ductility was correspondingly lower. Interestingly, Z values were comparable for both materials.

Large difference in strength was caused by different phase composition of L and H samples (see Figure 2). Structure of material L was composed of ferrite, martensite, bainite and pearlite (sorted from the most abundant to the rarest). Structure was heterogeneous. Ferrite content was 50 vol.% in the center, but increased towards the surfaces of the rolled sheets up to 75 vol.%. Pearlite was rare in the middle, but its content also rose towards the sheet surfaces. Difference between regimes 1 and 2 was observable only in pearlite content. Pearlite grains in regime 1 was up to 5 vol.% nearby the surface and only about 1 vol.% in case of regime 2. This can be caused by fast cooling of the surface area by contact with the rolls. Temperature could drop so low that pearlite transformation was not possible. Cooling was slower in the middle of the sheet and therefore pearlite transformation had time to start.

H samples were formed mostly by mixture of martensite, acicular ferrite and bainite with minor content of free polygonal ferritic grains. Structure was highly heterogeneous. Bands of pure martensite were present in the structure as well as narrow bands of ferritic grains. There was clear difference between regimes H 1 and H 2. Regime H1 resulted in mostly bainitic microstructure in whole thickness of the sheet. There was only small amount of free polygonal ferrite, most of the

ferrite was acicular or bainitic. Ferrite content was ca 25 vol.%. Regime H2 resulted in significant higher content of polygonal ferrite in vicinity of the sheet surface. Centre of the sheet was similar to the sample H1. Overall ferrite content was also ca 25 vol.%.

Table 3. Results of mechanical testing in as-rolled state. UTS – ultimate tensile strength, YS – yield stress at 0.2% offset, Ag – homogeneous plastic deformation, A5 – ductility, Z – reduction of area.

Regime	**UTS [MPa]**	**YS [MPa]**	**Ag [%]**	**A5 [%]**	**Z [%]**
L 1	1059	516	11.8	16.8	25
L 2	1084	533	10.0	14.2	20
H 1	1604	1158	2.9	8.6	23
H 2	1552	1048	4.0	7.0	16

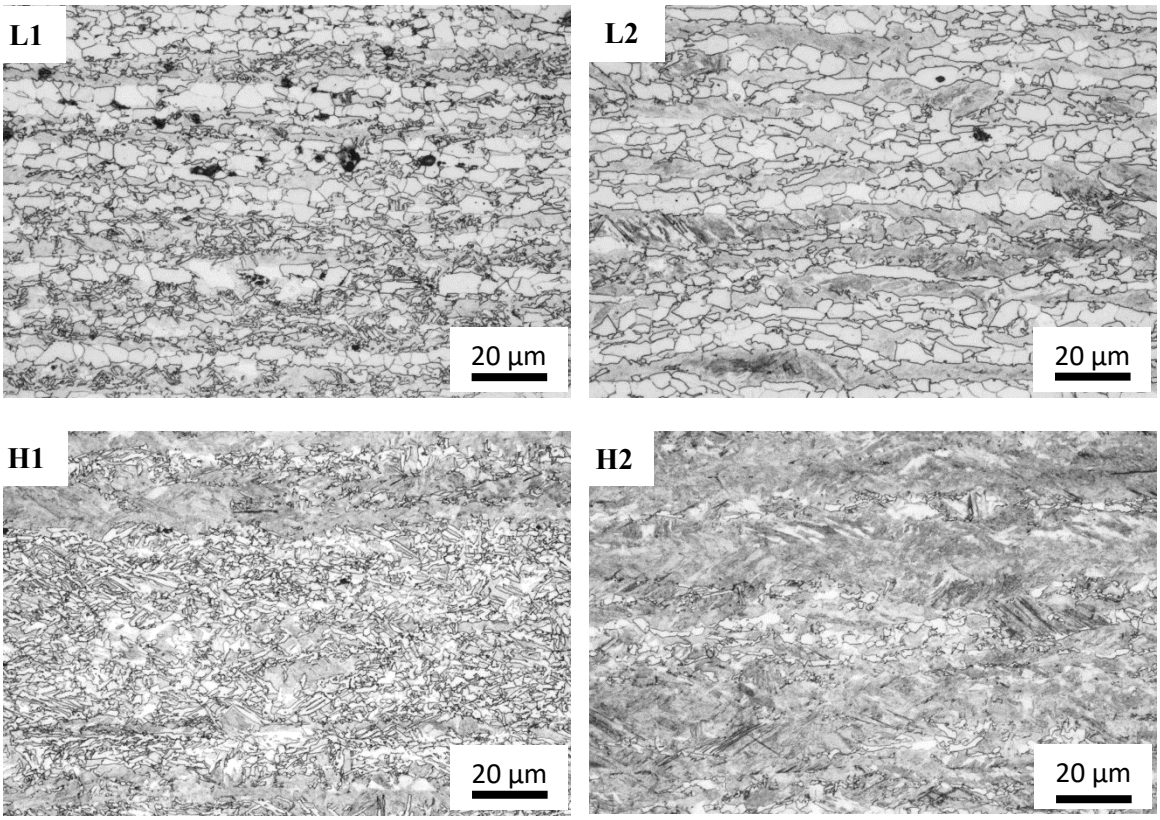

Figure 2. Micrographs of specimens in as-rolled state. Ferrite is white, martensite gray and pearlite forms dark areas (in L1 and L2)

Difference between materials L and H was not only in phase composition, but also in ferrite grain size (see Figure 3). Mostly polygonal ferrite grains in material L changed their diameter gradually from 8 µm in the center to 3 µm nearby the surface of the sheet. Polygonal ferrite grains in material H had size max. 3 µm, but most of the ferrite was acicular. Width of the ferrite plates was usually up to 2 µm, their length up to 10 µm. Acicular ferrite occurred in mixture with M/A islands. Large individual ferrite plates 1µm wide could be categorized as free acicular ferrite, but fine ferrite sheaves mixed with M/A plates fulfills definition of granular bainite.

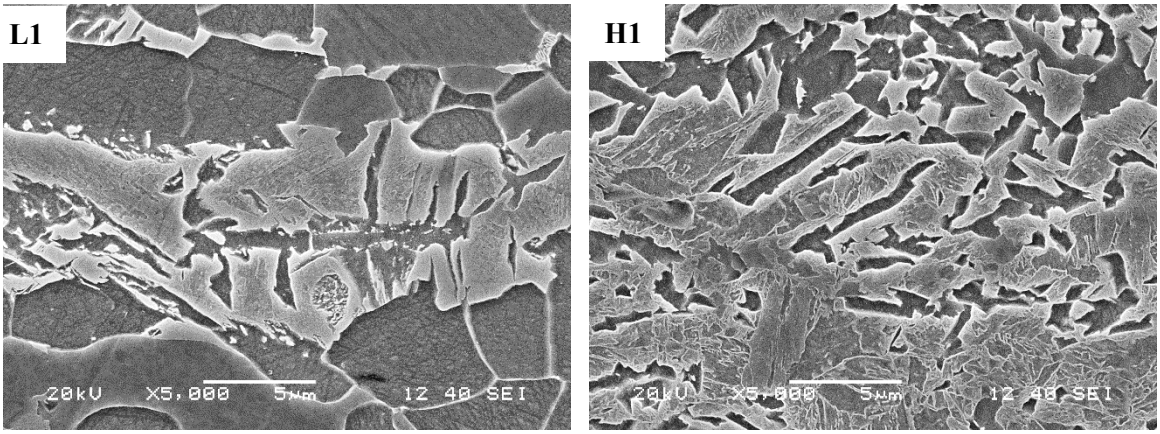

Figure 3. Micrographs of specimens in as-rolled state from SEM.

Annealing at 400°C for 60 minutes caused tempering of martensite and also provide favorable conditions for copper precipitation, as can be seen in Figure 4. Tempered martensite in materials L and H had different spatial density of precipitated carbides. It can be attributed to the higher carbon content of martensite in material L. There was less martensite in the material L compared to material H, thus all carbon remained concentrated in smaller volume. Carbon content in martensite was circa 0.4 wt.% for material L and 0.27 wt.% for material H based on estimated ferrite contents for these materials.
Copper precipitates cannot be identified by means of SEM analysis. Their observation can be only assumed on the basis of their appearance in literature. There were observed small particles less than 50 nm in diameter in ferrite in all samples. However, these particles were not well defined and clear in samples in as-rolled state. Much clearer were in the case of annealed samples, particularly in material L.

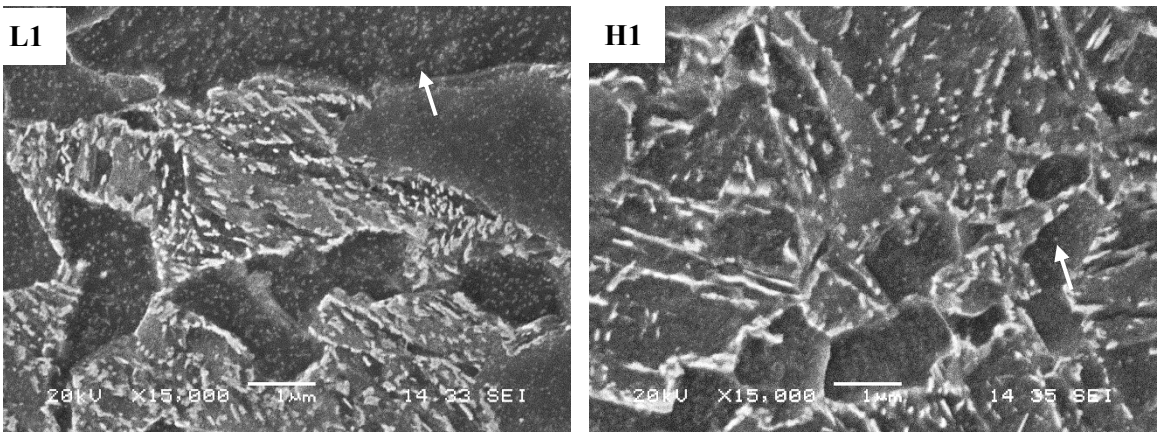

Figure 4. Micrographs of specimens in annealed state taken at higher magification. Aroows points to one of the particles in the ferrite, assumed to be copper precipitates.

Mechanical properties after annealing showed the same trend for all samples (see Table 4). YS increased and UTS decreased. In fact, they were almost identical for the material H. Material L retained more of the deformation hardening capability. Homogeneous plastic deformation slightly decreased in all cases, but ductility A5 increased as well as reduction of area. Also, there were much less difference between regimes 1 and 2 in comparison with as rolled state for both materials.

Table 4. Results of mechanical testing after annealing. Values of YS marked by asterisk (*) mean upper yield point. The specimens exhibited distinctive yield point in that case.

Regime	UTS [MPa]	YS [MPa]	Ag [%]	A5 [%]	Z [%]
L 1	839	785*	7.9	18.2	52
L 2	842	776*	7.8	18.6	48
H 1	1246	1231	2.6	11.8	40
H 2	1206	1186	2.6	10.8	47

Annealing also lead to the appearance of distinctive yield point in case of material L and to the sharp bend of material H stress-strain curve.

4 Conclusion

Complex-phase structure was prepared by controlled rolling. Prevailing ferritic-martensitic structure contained also small amount of bainite and pearlite. Alloying had strong effect on the resulting microstructure and properties. On the other hand, there was no significant difference upon changing final rolling temperature (FRT) from intercritical region between A3 and A1 to the subcritical temperature below A1. Both materials are favourable from the technological point of view because their properties does not depend strongly on FRT in examined range. There was significant heterogeneity observed between the centre and nearby the surface of sheets. Final thickness 5.6 mm was apparently too large and homogeneous structure could be achieved by rolling to thinner sheets.

Annealing at 400°C almost erased differences in sheet properties gained from rolling with different finish rolling temperatures. Copper precipitation might contribute to the significant rise of yield stress of ferritic-martensitic microstructure. It was accompanied by rapid decrease of deformation strengthening capability. Structure with approximate ferrite : martensite ratio 1:1 retained some of it, but structure with prevailing martensite exhibited almost none deformation strengthening after annealing.

Acknowledgements

The results presented in this paper arose under the project "Synergy of precipitation, deformation and transformation hardening in steels with higher copper content" No. 17-19002S funded by Czech Science Foundation.

These results were also created under the project entitled Development of West-Bohemian Centre of Materials and Metallurgy No.: LO1412, financed by the Ministry of Education, Youth and Sports of the Czech Republic.

References

[1] Takahashi, J., *et al.*, "Consideration of particle-strengthening mechanism of copper-precipitation-strengthened steels by atom probe tomography analysis," *Materials Science and Engineering A*, Vol. 532, (2012), pp. 144-152.

[2] Rana, R., *et al.*, "Development of high strength interstitial free steel by copper precipitation hardening," *Materials letters*, Vol. 61, (2007), pp. 2919-2922.

[3] Fine, M.E., *et al.*, "Origin of copper precipitation strengthening in steel revisited," *Scripta Materialia*, Vol. 53, (2005), pp. 115-118.

[4] Isheim, D., *et al.*, "An atom-probe tomographic study of the temporal evolution of the nanostructure of Fe–Cu based high-strength low-carbon steels," *Scripta Materialia*, Vol. 55, (2006), pp. 35-40.

[5] Podany, P. and Martinek, P. "Thermomechanical processing of micro-alloyed steel," *Materiali in Tehnologije*, Vol. 48, No. 6 (2014) pp. 855-859.

[6] Ghosh, S.K., *et al.*, "Effects of Cu addition on the synergistic effects of Ti–B in thermomechanically processed low carbon steels," *Materials Science and Engineering A*, Vol. 527, (2010), pp. 1082-1088.